



OPEN

## Isolation of circulating endothelial cells provides tool to determine endothelial cell senescence in blood samples

Katrin Kalies<sup>1✉</sup>, Kai Knöpp<sup>1</sup>, Leonie Wurmbrand<sup>1</sup>, Laura Korte<sup>2</sup>, Jochen Dutzmann<sup>1</sup>, Claudia Pilowski<sup>1</sup>, Susanne Koch<sup>1</sup> & Daniel Sedding<sup>1</sup>

Circulating endothelial cells (CEC) are arising as biomarkers for vascular diseases. However, whether they can be utilized as markers of endothelial cell (EC) senescence *in vivo* remains unknown. Here, we present a protocol to isolate circulating endothelial cells for a characterization of their senescent signature. Further, we characterize different models of EC senescence induction *in vitro* and show similar patterns of senescence being upregulated in CECs of aged patients as compared to young volunteers. Replication-(ageing), etoposide-(DNA damage) and angiotensin II-(ROS) induced senescence models showed the expected cell morphology and proliferation-reduction effects. Expression of senescence-associated secretory phenotype markers was specifically upregulated in replication-induced EC senescence. All models showed reduced telomere lengths and induction of the INK4a/ARF locus. Additional p14ARF-p21 pathway activation was observed in replication- and etoposide-induced EC senescence. Next, we established a combined magnetic activated- and fluorescence activated cell sorting (MACS-FACS) based protocol for CEC isolation. Interestingly, CECs isolated from aged volunteers showed similar senescence marker patterns as replication- and etoposide-induced senescence models. Here, we provide first proof of senescence in human blood derived circulating endothelial cells. These results hint towards an exciting future of using CECs as mirror cells for *in vivo* endothelial cell senescence, of particular interest in the context of endothelial dysfunction and cardiovascular diseases.

### Abbreviations

AngII	Angiotensin II
AT-1 receptor	Angiotensin II receptor type 1
BrdU	Bromodeoxyuridine
BSA	Bovine serum albumin
CAD	Coronary artery disease
CEC	Circulating endothelial cells
CVD	Cardiovascular disease
EC	Endothelial cell
EDTA	Ethylenediaminetetraacetic acid
EPC	Endothelial progenitor cells
FACS	Fluorescence activated cell sorting
γH2A.X	Phosphorylated histone H2A.X
HFpEF	Heart failure with preserved ejection fraction
HMGB-1	High mobility group box-1
HUVEC	Human umbilical vein endothelial cells
IL-1β	Interleukin-1 beta
IL-6	Interleukin-6

<sup>1</sup>Mid-German Heart Center, Department of Internal Medicine III, Division of Cardiology, Angiology and Intensive Medical Care, University Hospital Halle, Martin-Luther-University Halle-Wittenberg, Ernst-Grube-Strasse 40, 06120 Halle (Saale), Germany. <sup>2</sup>Department of Cardiology and Angiology, Hannover Medical School, Carl-Neuberg Straße 1, 30625 Hannover, Germany. ✉email: [katrin.kalies@uk-halle.de](mailto:katrin.kalies@uk-halle.de)

MACS	Magnetic beads associated cell sorting
NS	Non-senescent
PBS	Phosphate buffered saline
PDL	Passage doubling level
qRT-PCR	Quantitative real time polymerase chain reaction
RAGE	Receptor for advanced glycation endproducts
ROS	Reactive oxygen species
RS	Replicative senescent
SA- $\beta$ gal	Senescence-associated beta galactosidase
SASP	Senescence-associated secretory phenotype
SGLT-2	Sodium/glucose cotransporter-2
TLR	Toll-like receptor
TNF- $\alpha$	Tumor necrosis factor alpha
vWF	Von Willebrand factor

Endothelial cell senescence has been shown to contribute to endothelial dysfunction by accelerating the impairment of cellular function, barrier disruption and extracellular matrix degradation<sup>1</sup>. Senescence in general and in endothelial cells (EC) can be induced by multiple (patho-)physiological mechanism, including aging and age-related disorders<sup>2</sup>, chronic cellular stress (oxidative and mechanical)<sup>3–5</sup>, DNA damage (e.g. in cancer) or telomere shortening due to altered telomerase function (also frequently observed in cancer)<sup>6,7</sup>. Further, senescence-inducing factors might be therapy related as to chemotherapy or due to risk factors as smoking<sup>8,9</sup>. As such, studying EC senescence and its inducing mechanisms are of great interest to various research fields. However, the complex nature of senescent EC physiology, the magnitude of different cellular pathways involved and difficulties with accessing material for functional studies, complicates endothelial cell senescence research<sup>10,11</sup>.

In this regard, circulating endothelial cells (CEC) present a promising tool to further unravel EC characteristics. Currently exploited as biomarkers of EC function and cardiovascular disease (CVD) progression, CECs are emerging as easily accessible reflections of in vivo EC function<sup>12,13</sup>. CEC are defined as non-haematological cells with a mature endothelial identity and a limited growth capacity. They detach from the endothelium of the blood vessel wall after differentiation or vascular damage<sup>12,14</sup>. Thereby, CEC differ from endothelial progenitor cells (EPC) which are derived from the bone marrow to differentiate into mature endothelial cells and have a major role in vascular repair<sup>15</sup>. So far, the direct cell count of CEC has been exploited as a hint to the amount of endothelial damage<sup>16</sup>. However, the direct count displays a wide range in different studies due to different isolation protocols. Further, low CEC yield in human blood hampers CEC senescence research<sup>16</sup>. Previously published papers only agreed on the common expression of CD146 by CEC, sometimes accompanied by others among them CD45–, CD105+, vWF+, CD31+, CD133–, and CD34+<sup>17,18</sup>. Extending on this trend, we suggest CEC's to be usable as biomarkers of endothelial cell senescence and vascular ageing and thereby to endothelial dysfunction.

First, we here present a detailed characterization of endothelial cells in three different senescence models in vitro, namely replicative senescence, DNA-damage induced senescence and oxidative stress regarding their molecular features. In a next step we established a novel method of CEC isolation based on a combination of magnetic bead depletion (MACS) and fluorescence activated cell sorting (FACS) analysis to enumerate the cells enabling to provide first proof of CEC senescence in aged as compared to young volunteers.

## Methods

### Human material

Human EDTA-blood was collected from young volunteers and aged patients with CVD. Informed consent was obtained from all participants. The study was approved by the guidelines of the ethics committee from the Medical Faculty of the Martin-Luther-University Halle-Wittenberg (Registration number 2019-144) and performed according to the guidelines of the ethics committee from the Medical Faculty of the Martin-Luther-University Halle-Wittenberg and the Declaration of Helsinki. Isolated material was stored for further use. The probands were recruited by the University Hospital Halle, Department for Internal Medicine III. The healthy young participants were required to have a normal echocardiogram to meet the inclusion criteria, while the aged cohort (>60 years) needed either an abnormal echocardiogram or confirmation of CVD through a (prior) cardiac catheterization. Both groups were excluded if they had experienced an acute myocardial infarction or significant cardiovascular event within the past 3 months, were within 30 days after cardiopulmonary resuscitation, or if they had acute or chronic infectious diseases, along with concurrent autoimmune or tumor diseases. None of the probands underwent surgical interventions prior to blood collection. In total, 8 ml blood was collected in the morning and processed directly for further analysis.

### Cell culture and models of senescence

Human umbilical vein endothelial cells (HUVEC) were purchased from Lonza and cultivated in endothelial cell growth medium (PromoCell). All cells were maintained at 37 °C and 5% CO<sub>2</sub> in a humidified incubator, grown to confluency and passaged in a 1:3 ratio. For replication-induced senescence, passages <5 and >15 passages (Passage doubling level (PDL) <6 respectively >42) were considered. For treatment-induced senescence, cells of early passage numbers (<5) were treated either with 150  $\mu$ M Angiotensin II (AngII, 48 h) or with 100  $\mu$ M Etoposide (12 h).

### Isolation of RNA and quantitative real-time PCR (qRT-PCR)

Total RNA-isolation of cell culture samples was performed using the RNeasy Mini Kit together with the QIAshredder columns (Qiagen) following manufacturer's instruction. Cells were scraped in RLT-buffer, centrifuged over a shredder column and then transferred to an RNA-binding column. After several washing steps, RNA was eluted in Nuclease-free water. RNA measurement was performed using a nanodrop. RNA was transcribed to cDNA using the High Capacity cDNA Reverse Transcription kit (Applied Biosystems). For the qRT-PCR the Blue S'Green qPCR Kit from Biozym was used according to manufacturer's instruction. A list of used primers is shown in supplementary Table S1.

Total RNA-isolation of circulating endothelial cells from blood samples was performed using the miRNeasy micro Kit (Qiagen) following manufacturer's instructions for low cell counts. Briefly, cells were resuspended in Trizol, homogenized by vortexing, incubated for 5 min and then vigorously mixed with chloroform. After a short incubation step, samples were centrifuged for 15 min at 12,000×g at 4 °C to achieve a phase separation. The upper aqueous phase was transferred and thoroughly mixed with 1.5 volumes of 100% ethanol. The sample was then applied to an RNA-binding column. After several washing steps where the buffer was prepared with isopropanol instead of ethanol as well as an DNA digestion step, the spin column was washed with 80% ethanol. Followed by a short centrifugation step to dry the membrane, the RNA was eluted in Nuclease-free water.

### Determination of proliferation and telomere length

Proliferation was assessed by a Bromodeoxyuridine (BrdU) assay (Cell proliferation ELISA (colorimetric) (Roche)) according to the manufacturer's instructions. Further, live cell count was determined by life cell imaging. Therefore, cells were seeded into 96-well flat bottom plates. After cell adhesion, the plate was inserted into the life cell imaging system Cytation 1. Images were taken every 30 min for a 24-h period. Number of cells in the brightfield image were identified and counted automatically by the Gen5 software.

Genomic DNA was isolated from the cells by following the manufacturer's instructions of the GeneJET Genomic DNA Purification Kit (Thermo Fisher Scientific). Briefly, cells were diluted in lysis buffer with Proteinase K and incubated for 10 min at 56 °C. To ensure RNA digestion, RNase A was added for a prolonged cultivation time of 10 min at room temperature. Followed by the addition of 50% ethanol, the solution was transferred to a DNA purification column and centrifuged at 6000×g for 1 min. After several washing steps, the DNA was eluted. Further telomere length determination was performed using a Relative Human Telomere Length Quantification qPCR assay following manufacturer's instructions (ScienCell Research Laboratories).

### Senescence-associated $\beta$ -galactosidase (SA- $\beta$ -gal) staining

For the senescence-associated  $\beta$ -galactosidase staining we used a protocol previously published by Debacq<sup>19</sup>. For the colorimetric assay, cells were seeded on chamberslides to 50% confluency, fixed for 10 min and incubated over-night with an X-Gal staining solution.

### Immunofluorescence staining and morphometric analysis

For immunofluorescence staining's, cells were seeded to 80% confluency in 8-well microscopy slides. 24 h after seeding, cells were fixed for 30 min and blocked for 1 h. Staining with the primary antibody was performed overnight at 4 °C, the secondary antibody staining was conducted at room temperature for one hour. Cells were stained with DAPI and prepared for microscopy. Microscopic images were analyzed using ImageJ to evaluate cell size and nuclear size. Further information for the used antibodies can be found in Table S2.

### CEC isolation from human blood samples

First, the collected human EDTA-blood was subjected 1:20 to red blood cell lysis buffer (Biolegend) for 15 min. After centrifugation (345×g for 5 min), the cell pellet was resuspended in phosphate buffered saline (PBS) with 1% bovine serum albumin (BSA) and 1 mM Ethylenediaminetetraacetic acid (EDTA). In the following step, cells were incubated with CD45-magnetic beads for 15 min at 4 °C (Miltenyi Biotec), washed, and CD45 negative cells were depleted with LD-columns in the magnetic field of a MidiMACS-Separator (Miltenyi). Followed by an additional washing step, the effluent was subsequently stained with fluorescent labeled antibodies for CD45, CD11b, CD31, CD146 and CD34 (see supplementary Table S3). After 15 min of incubation at 4 °C in the dark, the sample was centrifuged, resuspended and sorted with a cell sorting system in the core facility of the University hospital Halle. CD45dim/CD11b-/CD31+/CD146+/CD34+ cells were defined as circulating endothelial cells. For further information on RNA and DNA isolation see above. For these analysis, cells were directly sorted into the corresponding lysis buffer. qRT-PCR analysis was performed as described above for mRNA expression analysis of endothelial cell and senescence markers as well as for telomere length determination. Additionally, freshly isolated endothelial cells were seeded on Fibronectin (2  $\mu$ g/cm<sup>2</sup>) and stained for endothelial cell markers, to confirm the gating strategy. Immunofluorescence staining was performed as described above.

### Statistical analysis

Statistical analysis of each experiment was performed with GraphpadPrism 8. All shown data are presented as mean  $\pm$  standard deviation, n indicates the number of individual experiments. Presented in vitro data are further color coded to the respective condition: replicative senescence in grey, Etoposide treatment in red and Angiotensin II treatment in blue. All datasets were normalized to their respective control. P < 0.05 was considered statistically significant. Differences between the study groups were analyzed by two-tailed unpaired Student's t-test.

## Results

### Senescent ECs present with reduced telomere lengths and heterogeneous SASP induction independent of EC senescence model used

The distinct role of senescent endothelial cells and their contribution to the development of endothelial dysfunction which in turn is involved in most cardiovascular pathologies is still under investigation. Oxidative stress, DNA damage and telomere stress (e.g. ageing) have been identified as main drivers of EC senescence, activating distinct cell cycle arrest mechanisms. As such, a multitude of methods to define senescent cells are currently described in literature. In order to establish relevant methods for EC senescence, we first evaluated standardly used methods of senescence detection for three distinct models of EC senescence: replication-induced, etoposide-induced and angiotensin II-induced EC senescence representing ageing, DNA damage and oxidative stress-induced senescence respectively.

In our hands, all models presented with the expected increased cell size and nuclear size, a flattened appearance as well as reduced proliferation as established by BrdU incorporation and cell count over time (Fig. 1A and B, data not shown). The detectable co-staining with the endothelial marker CD31 illustrates that also at higher passages, cells remain endothelial cells (Fig. 1). As described earlier<sup>19,20</sup>, beta-galactosidase positive cells accumulated in HUVECs at high passage numbers in the replication-induced EC senescence model (Fig. 1C).

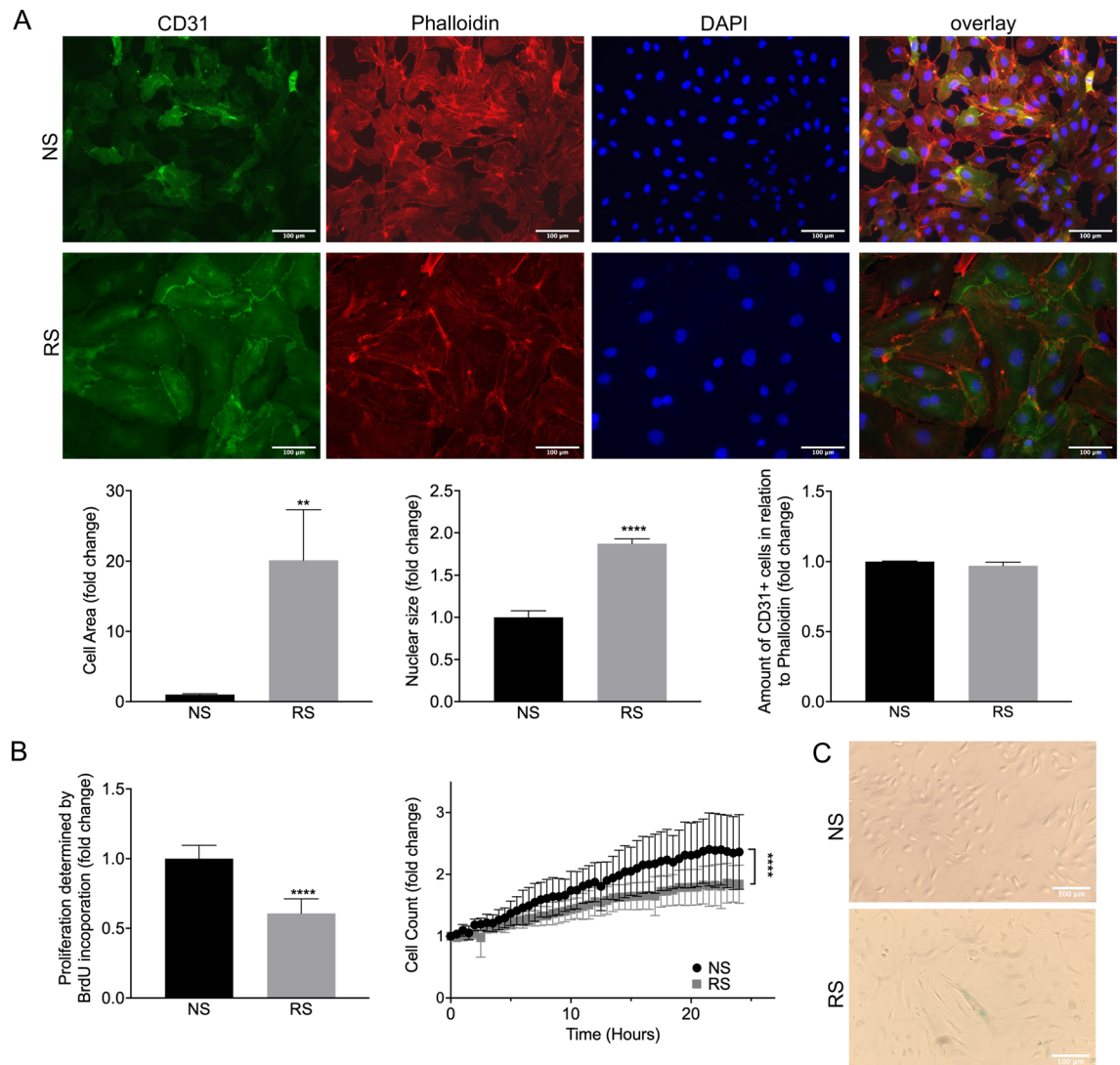


**Figure 1.** Replicative senescence (RS) on morphometric and proliferation scale. **(A)** Immunofluorescence staining of non-senescent (NS) and replicative senescent (RS) cells with staining for CD31 (green), Phalloidin (red) and DAPI (blue). Determination of cell area by measuring Phalloidin area in comparison to cell count.  $n = 3$  \*\* $P = 0.0018$ . Determination of nuclear size by measuring DAPI stained area.  $n = 3$  \*\*\*\* $P < 0.0001$ . Amount of CD31<sup>+</sup> cells in relation to Phalloidin stained cells  $n = 3$   $P = 0.1205$ . **(B)** Proliferation determined by BrdU incorporation.  $n = 3$  \*\*\*\* $P < 0.0001$ . Determination of proliferation by life cell imaging and cell counting over 24 h.  $n = 3$  \*\*\*\* $P < 0.0054$ . **(C)** Senescence-associated  $\beta$ -galactosidase staining. Replicative senescent cells are stained light blue.



Having established senescence induction on morphometric and proliferation scale, we further focused onto characterizing the distinct senescent pathways induced in these models.

The length of the telomere is an important criterion when studying cellular age. Also in our hands, telomere length decreased in replication-induced senescent endothelial cells and Ang II-treated cells and to a lesser extent in etoposide-treated HUVECs (Fig. 2A).

Next to arrested cell growth, the senescence-associated secretory phenotype (SASP) is a key characteristic of cellular senescence, promoting age-associated inflammation and pathology. This SASP is however heterogeneous, with the exact composition depending on senescence-inducer present. Also in our hands, we observe enhanced, yet heterogeneous, expression of SASP-associated genes tumor necrosis factor- $\alpha$  (TNF $\alpha$ ), Interleukin-1 beta (IL-1 $\beta$ ) and CD44<sup>21</sup> in all three EC senescence models tested, with etoposide treatment inducing most pronounced expression regulating effects. In turn, Interleukin-6 (IL-6) was specifically upregulated in replication-induced EC senescence only (Fig. 2B). In line with that, we observed decreased cellular presence

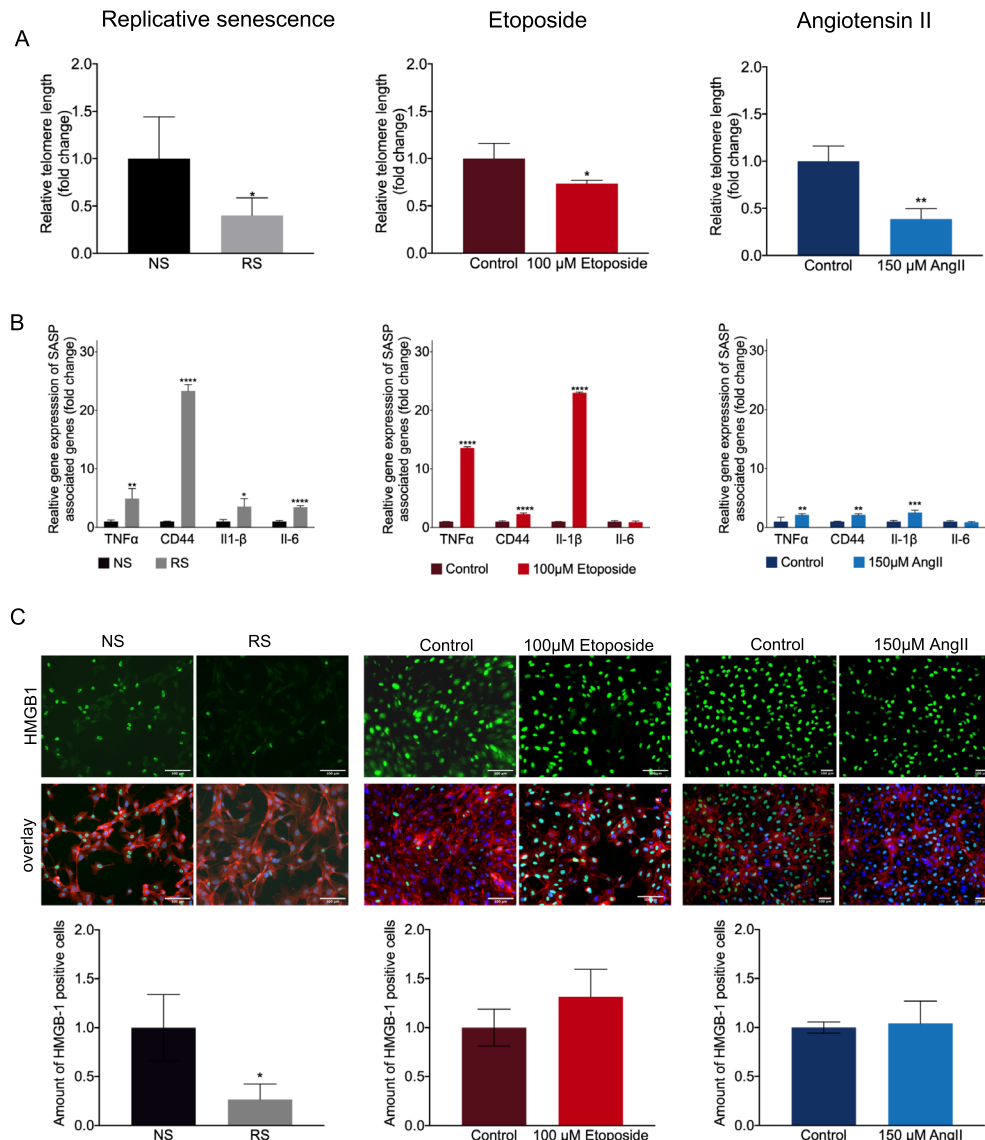


**Figure 2.** Measurement of telomere length, genes associated with the senescence-associated secretory phenotype and visualization of HMGB-1. (A) Quantification of relative telomere length by qRT-PCR analysis in replicative senescent (RS) cells.  $n = 3$   $^{*}P = 0.0201$ . Relative telomere length in the Etoposide-treated cells.  $n = 3$   $^{*}P = 0.0499$ . Relative telomere length in the angII-induced senescent cells.  $n = 3$   $^{*}P = 0.0054$ . (B) Relative gene expression level of CD44, TNF $\alpha$ , IL-1 $\beta$  and IL-6. Replicative senescent cells (RS)  $n = 3$  CD44  $^{****}P < 0.0001$ , TNF $\alpha$   $^{**}P = 0.0043$ , IL-1 $\beta$   $^{*}P = 0.0119$  and IL-6  $^{****}P < 0.0001$ . Etoposide-induced senescent cells.  $n = 3$  CD44  $^{****}P < 0.0001$ , TNF $\alpha$   $^{****}P < 0.0001$ , IL-1 $\beta$   $^{****}P < 0.0001$  and IL-6  $P = 0.8559$ . AngII-induced senescent cells.  $n = 3$  CD44  $^{**}P = 0.0025$ , TNF $\alpha$   $^{**}P = 0.0025$ , IL-1 $\beta$   $^{***}P = 0.0001$  and IL-6  $P = 0.9855$  (C) Immunofluorescence staining for HMGB-1 (green), Phalloidin (red) and DAPI (blue). Replicative senescent cells (RS).  $n = 3$   $^{*}P = 0.0274$ . Etoposide-induced senescent cells.  $n = 3$   $P = 0.1855$  AngII-induced senescent cells.  $n = 3$   $P = 0.7804$ .

of High mobility group box 1 (HMGB-1) as assessed by immunofluorescent staining in replication-induced senescent ECs (Fig. 2C). Upon senescence or cellular stress, HMGB-1 is shuffled into the extracellular space to where it binds amongst others cell surface to receptor for advanced glycation endproducts (RAGE) and toll-like receptors (TLRs) to initiate signaling, that results in expression of inflammatory cytokines including IL-6<sup>22,23</sup>. While we did not assess extracellular HMGB-1, we suggest that decreased cellular HMGB-1 observed here is likely reflecting increased shuffling of HMGB-1 into extracellular space, rather than reduced expression itself. For the other models a decreased presence of HMGB-1 was not observable.

### Replication- and etoposide-induced senescent ECs activate the p16INK4a cell cycle arrest pathway, while Ang II treatment likely acts via p14ARF-mediated senescence induction

Growth arrest was observed in all three models of EC induction, as illustrated earlier. Here, we assessed key cell cycle regulators involved in senescence induction in our three models, namely the INK4a/ARF locus and downstream p21 activation. Indeed, p16INK4a expression was elevated in replication-induced senescent ECs, a trend that could be confirmed on mRNA level for etoposide- and to a lesser extent for AngII treated cells (Fig. 3A). P14ARF induction was observed for replication-induced and etoposide-treated cells, but not for

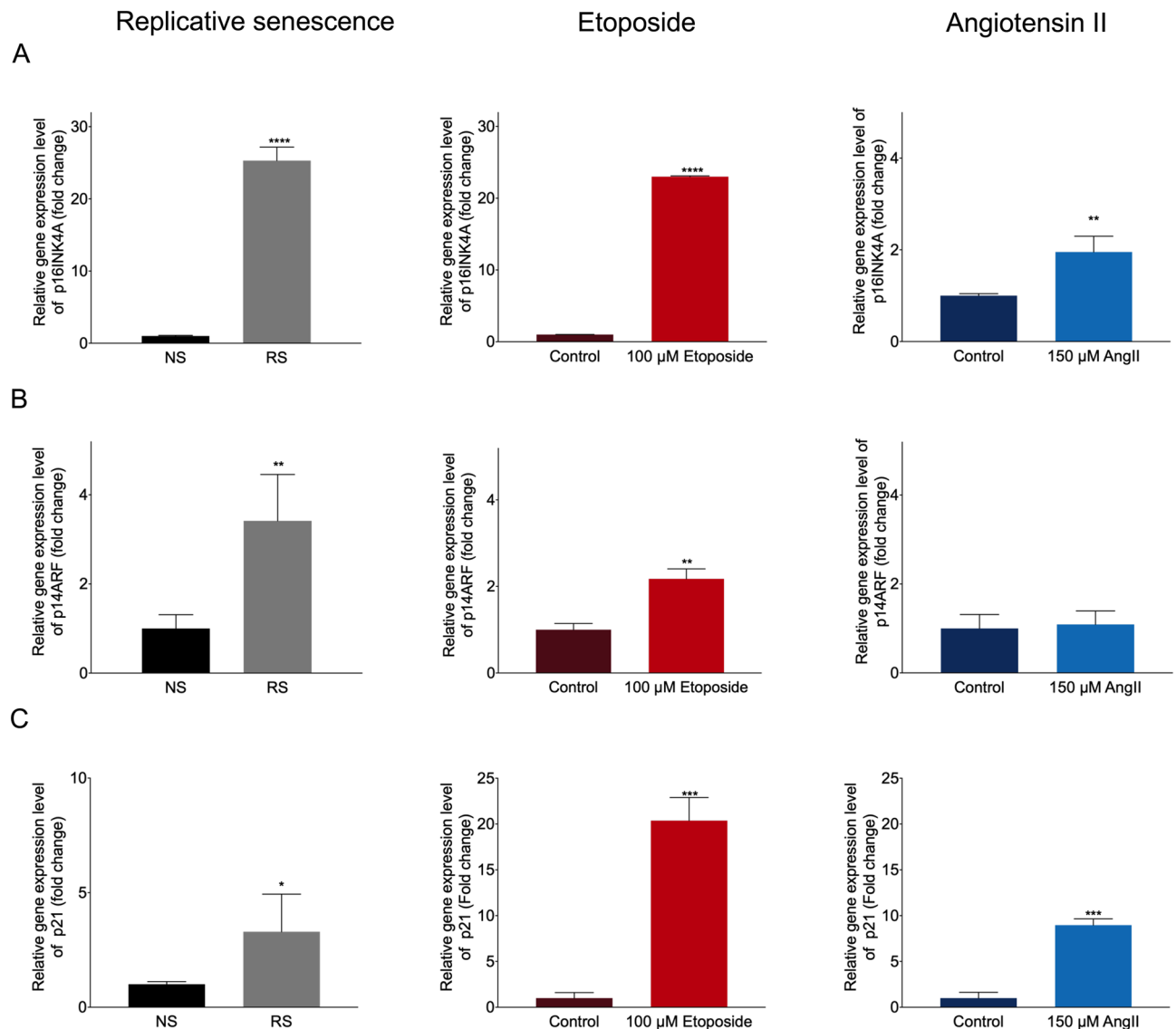


**Figure 3.** Quantification of cell cycle regulators p16INKA, p14ARF and p21 associated with cellular senescence. (A) Relative gene expression level of p16INK4A in all three models. Replicative senescent cells (RS)  $n = 3$  \*\*\*\* $P < 0.0001$ . Etoposide-induced senescent cells.  $n = 3$  \*\*\*\* $P < 0.0001$ . AngII-induced senescent cells.  $n = 3$  \*\* $P = 0.0088$ . (B) Relative gene expression level of p14ARF in all three models. Replicative senescent cells (RS).  $n = 3$  \*\* $P = 0.0044$ . Etoposide-induced senescent cells.  $n = 3$  \*\* $P = 0.0017$ . AngII-induced senescent cells.  $n = 3$   $P = 0.7376$ . (C) Relative gene expression level of p21 in all three models. Replicative senescent cells (RS).  $n = 3$  \* $P = 0.0317$ . Etoposide-induced senescent cells.  $n = 3$  \*\*\* $P = 0.0002$ . AngII-induced senescent cells.  $n = 3$  \*\*\* $P < 0.0001$ .

AngII-mediated senescence induction (Fig. 3B), indicating that this mainly oxidative stress-based model does not activate the p14ARF-p53-p21 cell arrest pathway. Yet, p21 was highly expressed in all three models, thus also AngII-treated cells (Fig. 3C), suggesting that p21 induction in AngII-treated cells is potentially independent of p14ARF induction.

Hinting towards a potential explanation, we observed increased DNA damage quantified as amount of histone H2A.X phosphorylation ( $\gamma$ H2A.X) present in cells, in replication-induced senescent ECs, complimentary to expected DNA damage in etoposide-treated cells (Fig. 4), suggesting that p14ARF pathway induction is potentially mainly observed in EC senescence models with excessive DNA-damage.

### CECs from elderly patients show increased levels of senescence marker

Next, we aimed to determine whether endothelial cell senescence can be detected in circulating endothelial cells, potentially reflecting in vivo endothelial dysfunction and vascular ageing. To this end, we first established a combined MACS-FACS-based CEC isolation protocol by integrating MACS-based CD45<sup>-</sup> cell selection combined with published and validated gating strategies of FACS<sup>13,24-26</sup> (live cell selection followed by CD45<sup>-</sup>, CD11b<sup>-</sup>, CD31<sup>+</sup>, CD34<sup>+</sup> and CD146<sup>+</sup> selection). In a first step, cells were labeled with CD45<sup>-</sup> magnetic beads and the CD45<sup>-</sup> cells were depleted by magnetic sorting. Subsequently CD45 negative cells resulting from MACS pre-selection, were FACS-sorted. Briefly, living cells determined by DAPI negative cells were used for a CD45 negative (incl. CD45<sup>dim</sup>) selection, followed by a CD11b negative population. With this cell fraction the further discrimination was performed by CD31/CD34 gating and CD31/CD146 gating (Fig. 5).

As validation of our protocol, these cells were plated on fibronectin-coated plates and stained for endothelial cell markers CD31, Von Willebrand factor (vWF) and CD146 (Supplemental Fig. 1). Attempts to cultivate the circulating endothelial cells from aged patients on fibronectin failed as they did not attach to the fibronectin coated plate whereas the cells from the young controls did attach. This observation already gives a hint on different rest functionality and might indicate differences in gene expression.

In total, CECs were isolated from 11 young volunteers and 11 aged patients with CVD comorbidities (Table 1). The young volunteers had an average age of 25.2 years, whereas the aged cohort was 73.5 years aged. All aged patients presented with at least presence of one CVD risk factor as smoking, diabetes, hypertension or hyperlipidemia. From the aged cohort, 10 participants were diagnosed for coronary artery disease (CAD) and all the participants in this cohort were treated for CVD, mostly with  $\beta$ -blockers, antiplatelet drugs and statine. In the young healthy cohort, all of the probands had a normal echocardiogram, however one proband was treated with Sodium/glucose cotransporter-2 (SGLT-2) inhibitors. Detected number of CEC had a low percentage on total viable cells of the MACS CD45<sup>+</sup> selection, but differed significantly in their general occurrence between the

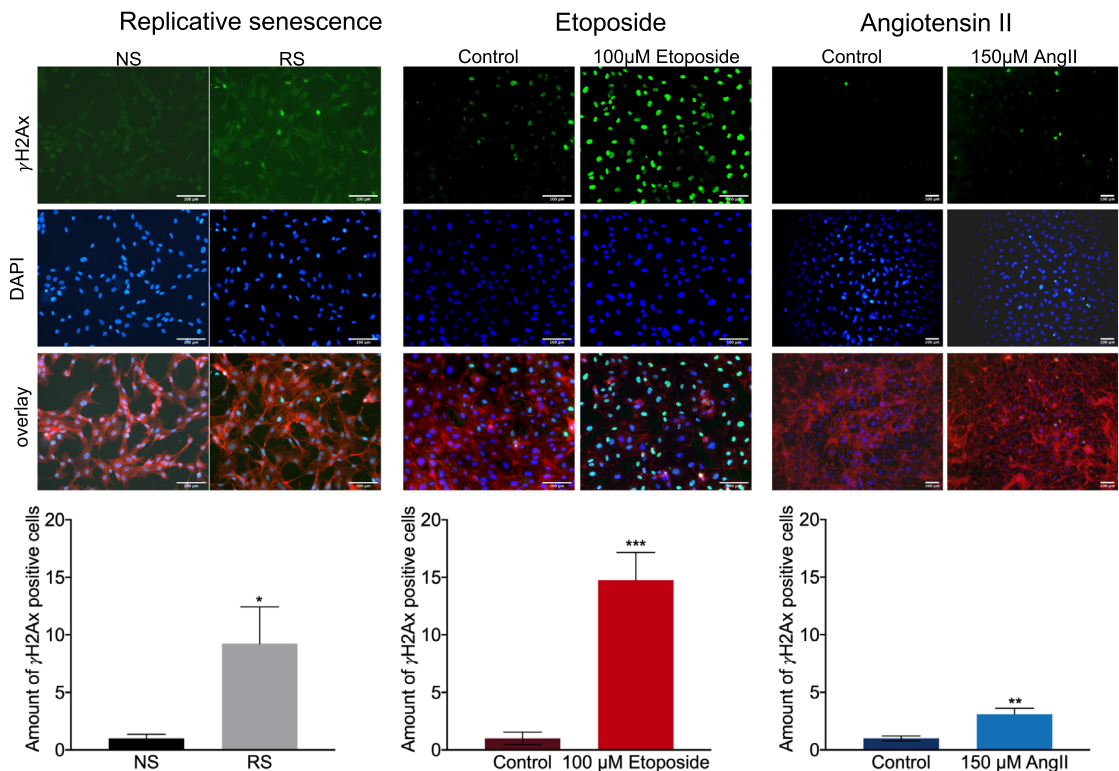


**Figure 4.** Impairment of cellular senescence on DNA damage. Immunofluorescent staining and quantification of  $\gamma$ H2Ax (green) positive cells, Phalloidin (red), DAPI (blue). Replicative senescent cells (RS). n = 3 \*\*\*\*P < 0.0001. Etoposide-induced senescent cells. n = 3 \*\*\*P = 0.0006. AngII-induced senescent cells. n = 3 \*\*P = 0.003.

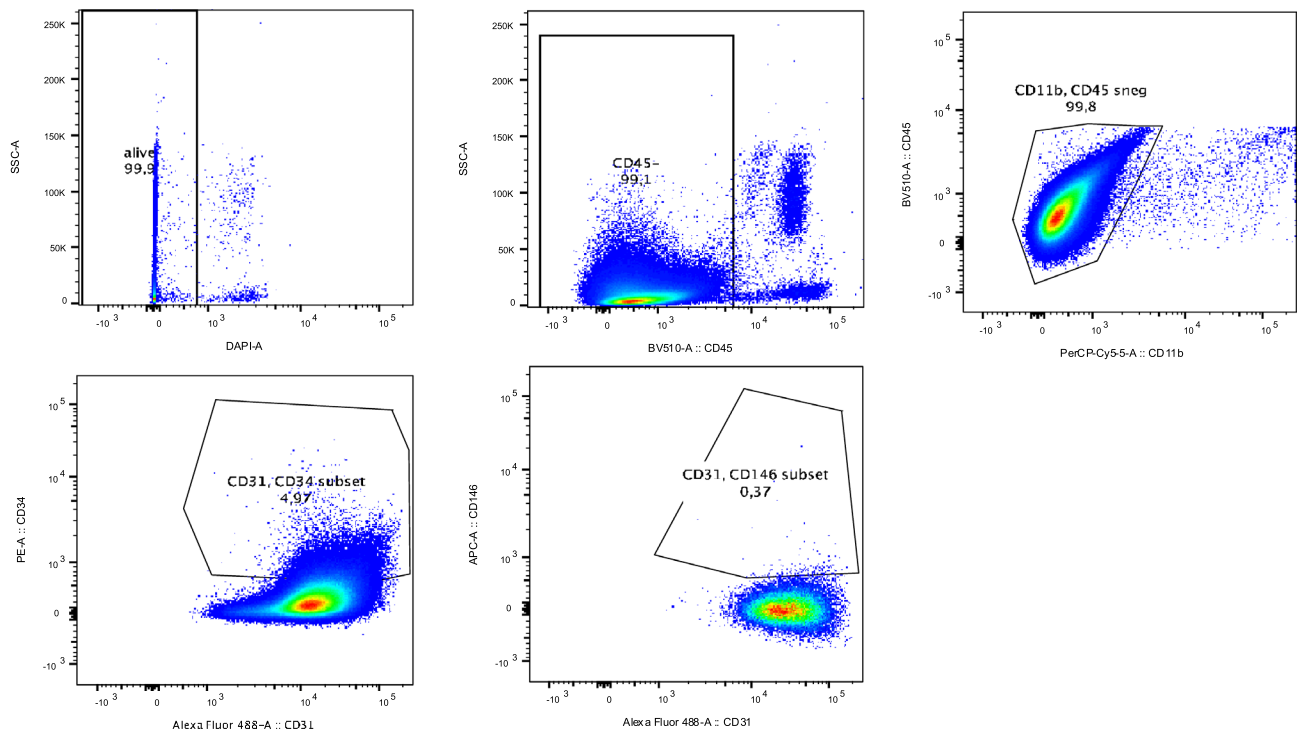


**Figure 5.** Isolation of circulating endothelial cells by combined selection with MACS-FACS-technology. Gating strategy for the FACS-analysis of circulating endothelial cells from human blood samples. Living cells were gated based on DAPI staining, followed by exclusion of CD45+ cells. After that, a gate for CD11b/CD45 was included. With this cell fraction the further discrimination was performed by CD31/CD34 gating and CD31/CD146 gating.

two groups. Total RNA and DNA-concentration in the CEC population did not differ between the two groups. Established protocols for DNA- and RNA-isolation ensured enough material for downstream analysis.

Having established various expression-based EC senescence markers *in vitro* (Figs. 2, 3), we next assessed these markers in CECs. Unfortunately, staining's and morphometric analyses were not possible on CECs due to difficulties with culturing ageing CECs from elderly volunteers. However, we could show that CECs from elderly people present with shortened telomeres, increased SASP-related gene expression signature (CD44 and TNF $\alpha$ ) and increased expression of cell cycle regulator genes p16ink4a, p21, but not p14ARF (Fig. 6).

With these experiments we could show that CEC can be isolated from blood samples and that these cells have an increased expression of senescence associated genes in the aged patients compared to the young controls.

## Discussion and conclusion

The complexity of EC senescence physiology as well as difficulties with accessing material for functional studies hampers EC senescence research in various fields.

Here, we provide first evidence of potential usability of circulating endothelial cells as reflections of vascular EC senescence, dysfunction and ageing. Employing a new combined MACS-and FACS-based CEC isolation method, we could isolate sufficient material to show increased EC senescence marker expression in elderly as compared to young individuals. The here observed results are displayed in Fig. 7, enabling to compare the observations from endothelial cell *in vitro* senescence to those characteristics observed in CEC.

The chosen *in vitro* models mimic different physiological stimuli that lead to cellular senescence: the replicative senescence reflects senescence observable during aging and is also known as cellular aging. The Etoposide model uses a chemotherapeutic that induces DNA-damage by interacting with topoisomerase II and thereby promoting DNA-double strand breaks<sup>27</sup>. In line with that DNA-damage effect, we observe high amount of  $\gamma$ H2Ax foci in this model. In contrast, the Ang II model was used to mimic oxidative stress-induced senescence and serves a physiological stimulus as it is a part of the renin-angiotensin system playing a role in cardiovascular dynamics, especially in vasoconstriction<sup>28,29</sup>. All these models have been used before to study cellular senescence<sup>30–33</sup>. However, we here present the first comprehensive comparison of the three models with regard to various senescence markers and characteristics: Morphological changes, inhibition of proliferation and SA- $\beta$ -gal-activity were observed for all models, as previously described in other cell types<sup>19,30–32,34–37</sup>. Also, the influence on the p53-p21 pathway was also already described for the models<sup>31,36</sup>. However, to our knowledge, we are the first to report release of HMGB-1 in replicative senescent cells but not in the other models. Upon senescence or cellular stress, HMGB-1 is shuffled into the extracellular space, where it binds amongst others cell surface RAGE and TLRs. This binding then initiates signaling, that results in expression of inflammatory cytokines including IL-6<sup>22,23</sup>. In line with that mechanism, we observe induction of IL-6 specifically in HMGB-1-releasing replicative



	Young (n = 11)	Old (n = 11)	p-value
Age	25.2 ( $\pm$ 2.72)	73.5 ( $\pm$ 11.36)	<0.0001
Sex			
f	81%	28%	
m	19%	72%	
BMI (kg/m <sup>2</sup> )	21.74 ( $\pm$ 1.6)	25.58 ( $\pm$ 2.5)	0.0005
Heart rate (bpm)	79 ( $\pm$ 9.4)	66.9 ( $\pm$ 8.3)	0.1807
Smoking (%)	9.1	45.5	
Diabetes (%)	0	54.5	
Hyperlipidaemia (%)	0	45.5	
Hypertension (%)	0	81.8	
CVD diagnosis (%)			
CAD	0	90.9	
Others	0	9.1	
LVEF (%)	62 ( $\pm$ 4.1))	55.3 ( $\pm$ 16.1)	0.2074
NT-pro BNP (ng/l)	<sup>a</sup>	1294.8 ( $\pm$ 1818.0)	
CRP (mg/l)	<sup>a</sup>	11.32 ( $\pm$ 17.9)	
LDL (mmol/l)	<sup>a</sup>	2.1 ( $\pm$ 0.9)	
Treatment no. (%)			
Antiplatelet drug	0	72.7	
ACE inhibitor	0	36.3	
$\beta$ -Blocker	0	90.9	
Diuretic	0	36.3	
Statine	0	72.7	
Metformin	0	36.4	
SGLT2 inhibitor	9.1	27.3	
Other CVD relevant	0	63.6	
CEC per ml blood	64.8 ( $\pm$ 84.5)	409.6 ( $\pm$ 418.1)	0.0217
% viable CEC on total cells after CD45+ MACS selection	0.0029 ( $\pm$ 0.005)	0.0007 ( $\pm$ 0.001)	0.1807
DNA concentration (ng/ $\mu$ l)	2.2 ( $\pm$ 1.1)	2.1 ( $\pm$ 2.3)	0.9606
RNA concentration (ng/ $\mu$ l)	17.5 ( $\pm$ 6.7)	18.4 ( $\pm$ 8.2)	0.7812

**Table 1.** Overview of characteristics of the cohort including clinical parameters as well as CEC count.

<sup>a</sup>Parameters not quantified.

senescent cells only. Release of HMGB-1 is mediated by the p53- pathway<sup>38</sup>. As this p53-pathway was fully upregulated in the etoposide model with an increased expression of p14ARF and p21, we suggest that HMGB-1 release is inhibited by other pathways in this setting. In turn, the lack of p14ARF regulation in the AngII model might explain the missing influence on HMGB-1 and IL-6.

In fact, AngII treatment likely induces EC senescence by a different pathway, namely activation of p21 through RAS rather than p14ARF<sup>39</sup>. AngII has previously been described to promote vascular senescence via an Angiotensin II receptor type 1 (AT1-receptor)-mediated inhibition of cyclin dependent kinase complexes and subsequent overexpression of p21<sup>28</sup>. In line with that, we observe increased p21 expression with unchanged p14ARF levels. However, the exact mechanism of p21 upregulation in our setting remains to be established. All these observations lead to the conclusion, that even though the models have many features in common, they also have major differences. This supports the need of choosing the right models to study senescence in a specific context.

The vascular endothelium in healthy humans is a dynamic barrier with a tight homeostasis of for example paracrine and autocrine regulators<sup>1,40,41</sup>. As soon as this tight homeostasis spins out of control, the endothelium becomes dysfunctional<sup>42</sup>. Often also observed in elderly, this endothelial dysfunction underlies clinical complications such as arterial stiffening or reduced endothelial-dependent dilation<sup>42</sup>. Recent histological studies show EC senescence in atherosclerotic plaques in individuals with ischemic heart disease, in the pathogenesis of heart failure, in aortic aneurysm, but also in aged healthy humans<sup>43–45</sup>. However, so far little is known about the exact role of EC senescence in CVD-related to the vasculature, except for that it is linked to a reduction in the regenerative and angiogenic capacity<sup>1</sup>.

Confirming earlier histological studies showing increased vascular EC senescence, we here observe enhanced expression of EC senescence markers in isolated circulating endothelial cells of elderly people.

Circulating cells in general are a new emerging field in the biomarker research, for example circulating tumor cells in certain cancer types<sup>46</sup>. In the vasculature, nonhematological circulating cells with endothelial identity can be detected, namely circulating endothelial cells<sup>14</sup>. These cells are released from the vasculature upon vascular damage<sup>12</sup> and can be linked to multiple disorders as myocardial infarction or heart failure with preserved ejection fraction (HFpEF)<sup>12,13</sup>. So far, the direct cell count of CEC has been used as a biomarker for

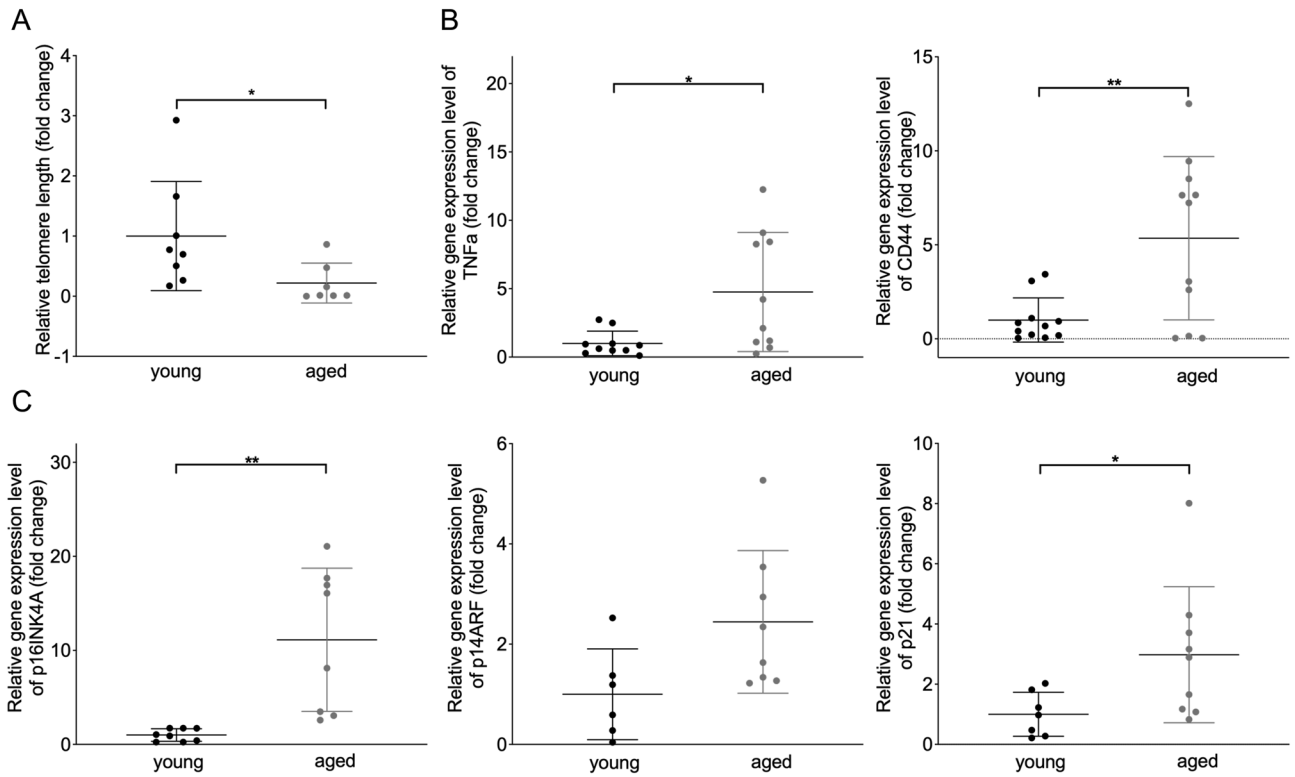


**Figure 6.** Quantification of senescence markers in circulating endothelial cells isolated from young individuals and aged patients with CVD. **(A)** Quantification of relative telomere length of young volunteers and aged individuals with CVD.  $n = 8$  \* $P = 0.0386$ . **(B–F)** Relative gene expression levels of CD44, TNF $\alpha$ , p16INK4A, p14ARF and p21 between young and aged individuals. CD44  $n = 11$  \*\* $P = 0.0044$ , TNF $\alpha$   $n = 10$  \* $P = 0.0156$ , p16INK4A  $n = 8$  \*\* $P = 0.0022$ , p14ARF  $n = 8$   $P = 0.0511$  and p21  $n = 9$  \* $P = 0.0441$ .

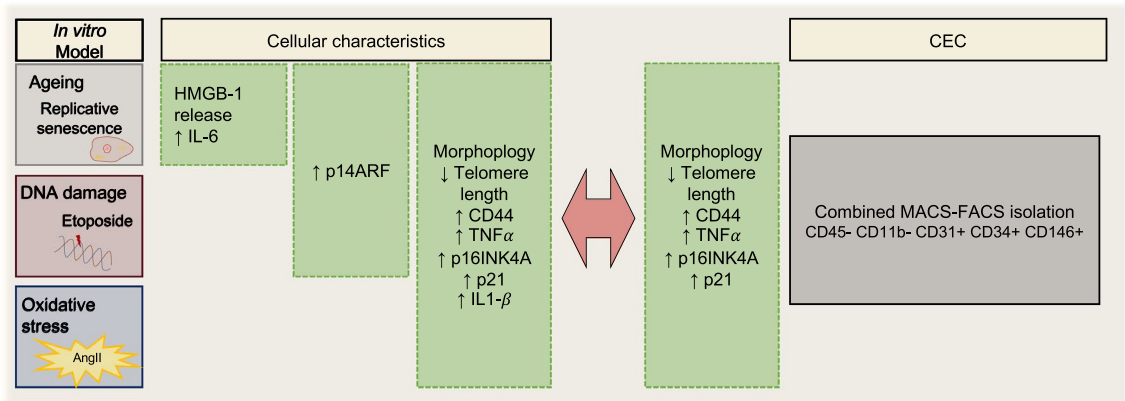


**Figure 7.** Summarizing observations.

endothelial damage, but between different studies a wide range of CEC counts in (healthy) individuals can be observed<sup>16</sup>. This wide range might on the one hand be explained by the very low cell numbers obtained, their heterogeneous phenotype and the diversity in approaches used to isolate CECs<sup>16</sup>. Our data reflect previous studies indicating higher CEC cell counts in diseased individuals than in young healthy controls in regard to total cell count<sup>12,13,16,47</sup>, but in the context of living cells, the counted CEC did not differ between the groups. The conclusion if the higher total count is based on disease presence or progression, the dysfunctionality of the endothelial cells or the age is limited by the absence of an age-matched healthy cohort as well as by the missing quantification of endothelial function of the participants of the study. However, rather than assessing sole CEC quantity, CEC characteristics should be integrated in current biomarker development efforts and consistent protocols for CEC isolation need to be established. Here, we present a first attempt of CEC characterization with regard to senescence marker assessment. As CEC and EC senescence can both be found in aged-individuals or CVDs, CEC senescence markers may not only provide (adjuvant) biomarker potential, but may even prove as

biologically relevant replicates of in vivo EC senescence, and present a valuable tool for functional studies and elucidate their role in the pathophysiology of CVDs.

In our study, we had access to aged volunteers with CVD co-morbidities and healthy young controls. The aged volunteers with CAD and HFpEF<sup>48,49</sup>, diseases associated with an endothelial dysfunction, presented with the expected CVD risk factors as smoking, hypertension or diabetes<sup>50</sup>. The established protocol to isolate CEC offers the great possibility to directly study this cell type in EDTA-blood samples. The combination of MACS-FACS-technology, described here, importantly enables a precise isolation. The CD45 negative pre-selection via MACS isolation removed among other cell types lymphocytes and leucocytes enabling the enrichment of CEC for FACS analysis. The selection used here also ensured to differentiate EPCs from CEC. Previous published protocols used a less stringent isolation<sup>12,13,16,47,51–53</sup>. The achieved RNA and DNA-quantity was sufficient to perform downstream analysis of some senescence-associated measurements. But, the inability of the cells to adhere as well as the low cell count prevented to perform all quantifications as in the in vitro models. Therefore, a conclusion whether senescence in CEC is replicative, related to DNA damage or oxidative stress is not possible as the obtained markers were commonly regulated in all three in vitro models and further investigations need to be conducted. Due to the low sample size (n = 11 aged volunteers and controls) and low material, we could not correct for co-morbidities in our analysis and cannot draw conclusions on whether EC senescence marker induction observed in elderly in this study is solely based on the age of the volunteers. A biased expression rather by CVD-comorbidities or even an interplay of both, age with CVD-comorbidities, is possible. To overcome this limitation, comparing with a group of elderly, healthy subjects would be meaningful, as it would allow differentiation between changes associated with aging and those associated with the disease. Further, an influence by either the risk factors or the CVD-treatment cannot be excluded as they are not present in the control group. In addition, it is known that some of treatments influence endothelial cell function. A therapy with Statin for example leads to increased levels of EPC<sup>54</sup>. Moreover, quantifying the endothelial dysfunction of the participants would allow conclusions to be drawn regarding whether the regulation of senescence-associated genes could also be related to the presence of endothelial dysfunction. While previous studies have shown a correlation between endothelial dysfunction and senescence, as well as between endothelial dysfunction and the occurrence of CEC, further connections have not yet been established<sup>13,21</sup>. Although the disease status and symptoms of the elderly, diseased patients with hypertension, diabetes, and CAD suggest the presence of endothelial dysfunction, this should be confirmed, for example, through measurement of the flow-mediated dilation in the forearm. This might further allow conclusions whether, CEC quantification and phenotyping as biomarker is more sensitive than the currently performed measurements. Yet, taken together our results provide first fundamental data for future research into CEC senescence to study not only their role in diseases, but also as a biomarker of in vivo EC function and vascular ageing or disease progression. Future studies should enable to focus on specific diseases. We further recommend to introduce an additional age-matched control group without CDV related co-morbidities to allow conclusions if the regulation is either age or disease related. The CEC isolation and genotyping might then present novel insights into vascular aging and the pathophysiology of diseases to use as biomarkers or develop possible treatment options.

In conclusion, we here provide first proof of CEC senescence detection in elderly as compared to young volunteers. This hints towards the exciting opportunity to exploit CEC senescence as potential reflection and biomarker of vascular endothelial function and ageing in vivo.

## Data availability

The datasets used and analyzed during the current study are available from the corresponding author on reasonable request.

Received: 24 August 2023; Accepted: 13 February 2024

Published online: 21 February 2024

## References

- Ungvari, Z., Tarantini, S., Donato, A. J., Galvan, V. & Csiszar, A. Mechanisms of vascular aging. *Circ. Res.* **123**, 849–867 (2018).
- North, B. J. & Sinclair, D. A. The intersection between aging and cardiovascular disease. *Circ. Res.* **110**, 1097–1108 (2012).
- Serrano, M., Lin, A. W., McCurrach, M. E., Beach, D. & Lowe, S. W. Oncogenic ras provokes premature cell senescence associated with accumulation of p53 and p16(INK4a). *Cell* **88**, 593–602 (1997).
- Toussaint, O., Medrano, E. E. & Von Zglinicki, T. Cellular and molecular mechanisms of stress-induced premature senescence (SIPS) of human diploid fibroblasts and melanocytes. *Exp. Gerontol.* **35**, 927–945. [https://doi.org/10.1016/S0531-5565\(00\)00180-7](https://doi.org/10.1016/S0531-5565(00)00180-7) (2000).
- Mallette, F. A., Gaumont-Leclerc, M. F. & Ferbeyre, G. The DNA damage signaling pathway is a critical mediator of oncogene-induced senescence. *Genes Dev.* **21**, 43–48 (2007).
- Allsopp, R. C. & Harley, C. B. Evidence for a critical telomere length in senescent human fibroblasts. *Exp. Cell Res.* **219**, 130–136 (1995).
- Harley, C. B., Futcher, A. B. & Greider, C. W. Telomeres shorten during ageing of human fibroblasts. *Nature* **345**, 458–460 (1990).
- Ahire, C. *et al.* Accelerated cerebrovascular senescence contributes to cognitive decline in a mouse model of paclitaxel (Taxol)-induced chemobrain. *Aging Cell* **22**, e13832 (2023).
- Childs, B. G., Durik, M., Baker, D. J. & van Deursen, J. M. Cellular senescence in aging and age-related disease: From mechanisms to therapy. *Nat. Med.* **21**, 1424–1435 (2015).
- Wang, A. S. & Dreesen, O. Biomarkers of cellular senescence and skin aging. *Front. Genet.* **9**, 1–14 (2018).
- Sharpless, N. E. & Sherr, C. J. Forging a signature of in vivo senescence. *Nat. Rev. Cancer* **15**, 397–408. <https://doi.org/10.1038/nrc3960> (2015).
- Boos, C. J., Lip, G. Y. H. & Blann, A. D. Circulating endothelial cells in cardiovascular disease. *J. Am. Coll. Cardiol.* **48**, 1538–1547. <https://doi.org/10.1016/j.jacc.2006.02.078> (2006).
- Farinacci, M. *et al.* Circulating endothelial cells as biomarker for cardiovascular diseases. *Res. Pract. Thromb. Haemost.* **3**, 49–58 (2019).

14. Lin, Y., Weisdorf, D. J., Solovey, A. & Heibel, R. P. Origins of circulating endothelial cells and endothelial outgrowth from blood. *J. Clin. Invest.* **105**, 71–77 (2000).
15. Pelliccia, F. *et al.* Endothelial progenitor cells in coronary artery disease: From bench to bedside. *Stem Cells Transl. Med.* **11**, 451–460 (2022).
16. Almici, C. *et al.* Circulating endothelial cell count: A reliable marker of endothelial damage in patients undergoing hematopoietic stem cell transplantation. *Bone Marrow Transplant.* **52**, 1637–1642 (2017).
17. Schmidt, D. E., Manca, M. & Hofer, I. E. Circulating endothelial cells in coronary artery disease and acute coronary syndrome. *Trends Cardiovasc. Med.* **25**, 578–587 (2015).
18. Kourek, C. *et al.* Exercise training effects on circulating endothelial and progenitor cells in heart failure. *J. Cardiovasc. Dev. Dis.* **9**, 222 (2022).
19. Debacq-Chainiaux, F., Erusalimsky, J. D., Campisi, J. & Toussaint, O. Protocols to detect senescence-associated beta-galactosidase (SA- $\beta$ gal) activity, a biomarker of senescent cells in culture and in vivo. *Nat. Protoc.* **4**, 1798–1806 (2009).
20. Dimri, G. P. *et al.* A biomarker that identifies senescent human cells in culture and in aging skin in vivo. *Proc. Natl. Acad. Sci.* **92**, 9363–9367 (1995).
21. Donato, A. J., Morgan, R. G., Walker, A. E. & Lesniewski, L. A. Cellular and molecular biology of aging endothelial cells. *J. Mol. Cell Cardiol.* **89**, 122–135 (2015).
22. Jong, S. P. *et al.* High mobility group box 1 protein interacts with multiple Toll-like receptors. *Am. J. Physiol. Cell Physiol.* **290**, 917–924 (2006).
23. Lotze, M. T. & Tracey, K. J. High-mobility group box 1 protein (HMGB1): Nuclear weapon in the immune arsenal. *Nat. Rev. Immunol.* **5**, 331–342. <https://doi.org/10.1038/nri1594> (2005).
24. Waldo, S. W. *et al.* A novel minimally-invasive method to sample human endothelial cells for molecular profiling. *PLoS ONE* **10**, e0118081 (2015).
25. Yu, S.-Y. *et al.* Methods in vascular biology isolation and characterization of human coronary artery-derived endothelial cells in vivo from patients undergoing percutaneous coronary interventions. *J. Vasc. Res.* **46**, 487–494 (2009).
26. Bogoslovsky, T. *et al.* Preservation and enumeration of endothelial progenitor and endothelial cells from peripheral blood for clinical trials. *Biomark. Med.* **9**, 625–637 (2015).
27. Yang, J. *et al.* Etoposide pathway. *Pharmacogenet. Genomics* **19**, 552–553 (2009).
28. Min, L. J., Mogi, M., Iwai, M. & Horiuchi, M. Signaling mechanisms of angiotensin II in regulating vascular senescence. *Ageing Res. Rev.* **8**, 113–121. <https://doi.org/10.1016/j.arr.2008.12.002> (2009).
29. Benigni, A., Cassis, P. & Remuzzi, G. Angiotensin II revisited: New roles in inflammation, immunology and aging. *EMBO Mol. Med.* **2**, 247–257. <https://doi.org/10.1002/emmm.201000080> (2010).
30. Petrova, N. V., Velichko, A. K., Razin, S. V. & Kantidze, O. L. Small molecule compounds that induce cellular senescence. *Ageing Cell* **15**, 999–1017 (2016).
31. Herbert, K. E. *et al.* Angiotensin II-mediated oxidative DNA damage accelerates cellular senescence in cultured human vascular smooth muscle cells via telomere-dependent and independent pathways. *Circ. Res.* **102**, 201–208 (2008).
32. Shan, H. Y., Bai, X. J. & Chen, X. M. Apoptosis is involved in the senescence of endothelial cells induced by angiotensin II. *Cell Biol. Int.* **32**, 264–270 (2008).
33. Shan, H., Bai, X. & Chen, X. Angiotensin II induces endothelial cell senescence via the activation of mitogen-activated protein kinases. *Cell Biochem. Funct.* **26**, 459–466 (2008).
34. Campisi, J. & D'Adda Di Fagagna, F. Cellular senescence: When bad things happen to good cells. *Nat. Rev. Mol. Cell Biol.* **8**, 729–740 (2007).
35. Hayflick, L. The limited in vitro lifetime of human diploid cell strains. *Exp. Cell Res.* **37**, 614–636 (1965).
36. Litwiniec, A., Gackowska, L., Helmin-Basa, A., Żuryń, A. & Grzanka, A. Low-dose etoposide-treatment induces endoreplication and cell death accompanied by cytoskeletal alterations in A549 cells: Does the response involve senescence? The possible role of vimentin. *Cancer Cell Int.* **13**, 9 (2013).
37. Robin, V., Wang, Y., Bai, A. & Zhou, D. Busulfan selectively induces cellular senescence but not apoptosis in WI38 fibroblasts via a p53-independent but extracellular signal-regulated kinase-p38 mitogen-activated protein kinase-dependent mechanism. *J. Pharmacol. Exp. Ther.* **319**, 551–560 (2006).
38. Davalos, A. R. *et al.* p53-dependent release of Alarmin HMGB1 is a central mediator of senescent phenotypes. *J. Cell Biol.* **201**, 613–629 (2013).
39. Wei, W., Hemmer, R. M. & Sedivy, J. M. Role of p14ARF in replicative and induced senescence of human fibroblasts. *Mol. Cell Biol.* **21**, 6748–6757 (2001).
40. Brandes, R. P., Fleming, I. & Busse, R. Endothelial aging. *Cardiovasc. Res.* **66**, 286–294. <https://doi.org/10.1016/j.cardiores.2004.12.027> (2005).
41. Mistriotis, P. & Andreadis, S. T. Vascular aging: Molecular mechanisms and potential treatments for vascular rejuvenation. *Ageing Res. Rev.* **37**, 94–116. <https://doi.org/10.1016/j.arr.2017.05.006> (2017).
42. Donato, A. J., Machin, D. R. & Lesniewski, L. A. Mechanisms of dysfunction in the aging vasculature and role in age-related disease. *Circ. Res.* **123**, 825–848 (2018).
43. Minamino, T. *et al.* Endothelial cell senescence in human atherosclerosis: Role of telomere in endothelial dysfunction. *Circulation* **105**, 1541–1544 (2002).
44. Gevaert, A. B., Lemmens, K., Vrints, C. J. & Van Craenenbroeck, E. M. Targeting endothelial function to treat heart failure with preserved ejection fraction: The promise of exercise training. *Oxid. Med. Cell Longev.* **2017**, 1–17 (2017).
45. Cafueri, G. *et al.* Endothelial and smooth muscle cells from abdominal aortic aneurysm have increased oxidative stress and telomere attrition. *PLoS ONE* **7**, e35312 (2012).
46. Danila, D. C., Pantel, K., Fleisher, M. & Scher, H. I. Circulating tumor cells as biomarkers: Progress toward biomarker qualification. *Cancer J.* **17**, 438–450. <https://doi.org/10.1097/PPO.0b013e31823e69ac> (2011).
47. Martínez-Sales, V. *et al.* Circulating endothelial cells in patients with heart failure and left ventricular dysfunction. *Dis. Markers* **31**, 75–82 (2011).
48. Shao, C., Wang, J., Tian, J. & da Tang, Y. Coronary artery disease: From mechanism to clinical practice. *Adv. Exp. Med. Biol.* **1177**, 1–36 (2020).
49. Cornuault, L., Rouault, P., Dupl a, C., Couffinal, T. & Renault, M. A. Endothelial dysfunction in heart failure with preserved ejection fraction: What are the experimental proofs?. *Front. Physiol.* **13**, 906272 (2022).
50. 2021 ESC Guidelines on cardiovascular disease prevention in clinical practice | European Heart Journal | Oxford Academic. <https://academic.oup.com/eurheartj/article/42/34/3227/6358713?login=true#371852138>.
51. Lee, K. W., Lip, G. Y. H., Tayebjee, M., Foster, W. & Blann, A. D. Circulating endothelial cells, von Willebrand factor, interleukin-6, and prognosis in patients with acute coronary syndromes. *Blood* **105**, 526–532 (2005).
52. Freestone, B. *et al.* Circulating endothelial cells in atrial fibrillation with and without acute cardiovascular disease. *Thromb. Haemost.* **94**, 702–706 (2005).
53. Quilici, J. *et al.* Circulating endothelial cell count as a diagnostic marker for non-ST-elevation acute coronary syndromes. *Circulation* **110**, 1586–1591 (2004).



54. Vasa, M. *et al.* Increase in circulating endothelial progenitor cells by statin therapy in patients with stable coronary artery disease. *Circulation* **103**, 2885–2890 (2001).

### Author contributions

K.K., K.Kn., J.D. and D.S. designed the study and supervised this project. K.K., K.Kn., L.W., L.K., S.K. and C.P. performed experiments. K.K. and K.Kn. analyzed the data. K.K. wrote the manuscript. All authors read and approved the final manuscript.

### Funding

Open Access funding enabled and organized by Projekt DEAL.

### Competing interests

The authors declare no competing interests.

### Additional information

**Supplementary Information** The online version contains supplementary material available at <https://doi.org/10.1038/s41598-024-54455-5>.

**Correspondence** and requests for materials should be addressed to K.K.

**Reprints and permissions information** is available at [www.nature.com/reprints](http://www.nature.com/reprints).

**Publisher's note** Springer Nature remains neutral with regard to jurisdictional claims in published maps and institutional affiliations.



**Open Access** This article is licensed under a Creative Commons Attribution 4.0 International License, which permits use, sharing, adaptation, distribution and reproduction in any medium or format, as long as you give appropriate credit to the original author(s) and the source, provide a link to the Creative Commons licence, and indicate if changes were made. The images or other third party material in this article are included in the article's Creative Commons licence, unless indicated otherwise in a credit line to the material. If material is not included in the article's Creative Commons licence and your intended use is not permitted by statutory regulation or exceeds the permitted use, you will need to obtain permission directly from the copyright holder. To view a copy of this licence, visit <http://creativecommons.org/licenses/by/4.0/>.

© The Author(s) 2024